processes

MDPI

Article

Synthesis of 2-(4-hydroxyphenyl)ethyl 3,4,5-Trihydroxybenzoate and Its Inhibitory Effect on Sucrase and Maltase

Wen-Tai Li [1,†], Yu-Hsuan Chuang [2,†], Jiahn-Haur Liao [3,†] and Jung-Feng Hsieh [2,4,*]

1 National Research Institute of Chinese Medicine, Ministry of Health and Welfare, Taipei 112, Taiwan; lwt0220@nricm.edu.tw
2 Department of Food Science, Fu Jen Catholic University, New Taipei City 242, Taiwan; d88320001@pchome.com.tw
3 Institute of Biological Chemistry, Academia Sinica, Taipei 115, Taiwan; b826141@gmail.com
4 Ph.D. Program in Nutrition & Food Science, Fu Jen Catholic University, New Taipei City 242, Taiwan
* Correspondence: 075101@mail.fju.edu.tw; Tel.: +886-2-2905-2516
† These authors contributed equally to the work.

Received: 29 October 2020; Accepted: 3 December 2020; Published: 5 December 2020

Abstract: We report on the synthesis of an active component, 2-(4-hydroxyphenyl)ethyl 3,4,5-trihydroxybenzoate (HETB), from *Rhodiola crenulata*. Subsequent analysis revealed that HETB exhibits α-glucosidase inhibitory activities on maltase and sucrase, with potency exceeding that of the known α-glucosidase inhibitors (voglibose and acarbose). An inhibition kinetics study revealed that HETB, acarbose, and voglibose bind to maltase and sucrase, and HETB was shown to be a strong competitive inhibitor of maltase and sucrase. In a molecular docking study based on the crystal structure of α-glucosidase from *Saccharomyces cerevisiae*, we revealed the HETB binding in the active site of maltase via hydrogen-bond interactions with five amino acid residues: Ser 240, Asp 242, Glu 277, Arg 315, and Asn 350. For HETB docked to the sucrase active site, seven hydrogen bonds (with Asn 114, Glu 148, Gln 201, Asn 228, Gln 381, Ile 383, and Ser 412) were shown.

Keywords: kinetics assay; sucrase; maltase; hyperglycemia; inhibitor

1. Introduction

Changes in food habits and population aging have led to an expansion in the occurrence of diabetes [1]. Defects in the regulation of insulin secretion manifest as endocrine and metabolic dysregulation in the form of chronic hyperglycemia, dyslipidemia, and disorders of protein metabolism [2]. The prolonged increment in blood glucose concentrations during the postprandial period of diabetes mellitus can be countered by inhibiting α-glucosidases, thereby delaying starch digestion and decreasing the rate of glucose absorption [3,4]. α-Glucosidase inhibitors, for example, voglibose and acarbose, have been shown to limit diabetes progression [5]. The key enzyme catalyzing the last stage of starch metabolism is α-glucosidase situated in the striated border surface layer of intestinal small intestinal cells [6].

During digestion, α-glucosidases (EC 3.2.1.20) are involved in hydrolyzing terminal nonreducing 1-4-linked α-glucose residues, bringing about the arrival of glucose molecules. α-glucosidases can be divided into four types of hydrolases: isomaltase (EC 3.2.1.10), sucrase (EC 3.2.1.48), glucoamylase (EC 3.2.1.3), and maltase (EC 3.2.0.20). The four enzymes release glucose after reaction with disaccharide or polysaccharide. Among them, sucrase and maltase can hydrolyze sucrose and maltose derived from dietary starch, respectively [6]. Maltase is an enzyme that breaks down the disaccharide maltose, it can hydrolyze the α-1,4-linkages of maltose, resulting in the release of glucose [7]. Furthermore, sucrase

is an important disaccharidase, which can hydrolyze sucrose to glucose and fructose monomeric units [8,9]. After a mixed carbohydrate diet, the inhibition of maltase and sucrase can decrease the postprandial increment of blood glucose.

The current treatment strategy to control postprandial hyperglycemia is to inhibit α-glucosidase (maltase and sucrase), resulting in digestive delay of carbohydrates and thus the absorption of glucose [10]. Miglitol, acarbose, voglibose, and emiglitate are known α-glucosidase inhibitors capable of hindering diabetes progression [5]. Voglibose and acarbose are the most widely used α-glucosidase inhibitors for the treatment of diabetes, due in part to the fact that they are not consumed by the gastrointestinal tract after oral administration and therefore pose a lower risk of hypoglycemia [11,12]. In the previous study, we purified and characterized HETB as an α-glucosidase inhibitor from *Rhodiola crenulata* [13].

The use of potent sucrase and maltase inhibitors have been considered to treat diabetes mellitus [14]. The inhibitory properties of HETB on α-glucosidase have previously been reported. However, the inhibitory effect of HETB on maltase and sucrase has not been examined. Following the synthesis of HETB, we investigated the inhibitory properties of acarbose, voglibose, and HETB on maltase and sucrase. The point of this investigation was to examine the inhibitory properties of HETB and its intermediate compounds on sucrase and maltase.

2. Materials and Methods

2.1. Synthesis of 2-(4-hydroxyphenethyl)enyl 3,4,5-trihydroxybenzoate (HETB)

2.1.1. Synthesis of 2-[4-(benzyloxy)phenyl]ethanol (3)

4-(2-Hydroxyethyl)phenol (compound 1, Sigma Chemical Co., St. Louis, MO, USA) (36.2 mmol, 5.0 g) was added into a mixture of benzyl bromide (compound 2, Sigma Chemical Co., St. Louis, MO, USA) (36.2 mmol, 8.9 mL) and potassium carbonate (54.3 mmol, 7.5 g) in ethanol (25.0 mL). The reaction mixture underwent stirring until the reactions were completed (12 h), as determined by thin-layer chromatography (TLC) monitoring. Silica gel column chromatography was used to purify the residue, which resulted in the formation of compound 3 as a white solid (6.2 g, yield: 75%). ^{1}H-nuclear magnetic resonance spectroscopy (^{1}H-NMR) (400 MHz, $CDCl_3$): δ 2.80 (2 H, t, J = 6.4, 6.6 Hz, H-7), 3.81 (2 H, t, J = 6.4 Hz, H-8), 5.03 (2 H, s, H-7′), 6.91 (2 H, d, J = 8.4 Hz, H-3, 5), 7.13 (2 H, d, J = 8.8 Hz, H-2, 6), 7.36 (5 H, m, H-2′-6′) ppm; electrospray ionization mass spectrometry (ESIMS) m/z 228.1 $[M]^+$.

2.1.2. Synthesis of methyl 3,4,5-tris(benzyloxy)benzoate (5)

A mixture of methyl 3,4,5-trihydroxybenzoate (compound 4, 2.0 g, 10.9 mmol), benzyl bromide (compound 2, 8.5 mL, 34.8 mmol), and potassium carbonate (6.0 g, 43.4 mmol) in acetone (35 mL) was heated to reflux for 5 h. The mixture was filtered, and the solvent was removed to give 5 as a white solid (4.9 g, yield: 99%). ^{1}H-NMR (600 MHz, $CDCl_3$): δ 3.88 (3 H, s, H-8), 5.12 (2 H, s, H-7″), 5.13 (4 H, s, H-7′, 7‴), 7.34 (17 H, m, H-2, 6, 2′-6′, 2″-6″, 2‴-6‴) ppm; ESIMS m/z 476.75 $[M + Na]^+$.

2.1.3. Synthesis of 3,4,5-tris(benzyloxy)benzoic acid (6)

Compound 5 (4.9 g, 10.8 mmol) and potassium hydroxide (0.9 g, 16.0 mmol) in tetrahydrofuran (THF)/H_2O (v:v = 1:1, 44 mL) were heated to reflux for 1 h. After cooling, the mixture was poured into a mixture of ice and cold water, and 2 N aqueous HCl was added slowly until the mixture was at pH = 1. Ethyl acetate was used to extract the aqueous phase, whereupon the combined organic material underwent drying, filtering, and concentration under vacuum to produce compound 6 as a white solid (4.5 g, yield: 95%). 1H-NMR (400 MHz, CDCl3): δ 5.12 (2 H, s, H-7″), 5.13 (4 H, s, H-7′, 7‴), 7.34 (17 H, m, H-2, 6, 2′-6′, 2″-6″, 2‴-6‴) ppm; ESIMS m/z 439.06 $[M–H]^-$.

2.1.4. Synthesis of 4-phenoxyphenethyl 3,4,5-triphenoxybenzoate (7)

A mixture of 2-[4-(benzyloxy)phenyl]ethanol 3 (6.2 g, 27.2 mmol), 3,4,5-tris(benzyloxy)benzoic acid 6 (4.5 g, 10.2 mmol), 4-dimethylaminopyridine (0.5 g, 4.1 mmol), *N*,*N*′-dicyclohexylcarbodiimide (5.58 g, 27.0 mmol), and Et_3N (11.4 mL) in THF (270 mL) was stirred for 3 days, when reaction was complete, as judged by TLC. The residue was purified by silica gel column chromatography to give 7 as a white solid (9.3 g, yield: 54%). ^{1}H-NMR (600 MHz, $CDCl_3$): δ 2.98 (2 H, t, *J* = 6.9, 7.2 Hz, H_B-7), 4.44 (2 H, t, *J* = 6.6, 6.9 Hz, H_B-8), 5.10 (2 H, s, H_A-7″), 5.10 (4 H, s, H_A-7′, 7‴), 6.92 (2 H, d, *J* = 8.4 Hz, H_B-3, 5), 7.17 (2 H, d, *J* = 8.4 Hz, H_B-2, 6), 7.31 (22 H, m, H_A-2, 6, 2′-6′, 2″-6″, 2‴-6‴; H_B-2′-6′) ppm; ESIMS m/z 672.96 $[M + Na]^+$.

2.1.5. Synthesis of 2-(4-hydroxyphenethyl)enyl 3,4,5-triphenoxybenzoate (HETB)

4-Phenoxyphenethyl 3,4,5-triphenoxybenzoate 7 (9.3 g, 14.3 mmol) was added into a mixture of palladium on carbon (0.46 g) in methanol (143 mL). The solution was stirred for 3 days in hydrogen gas. The reaction mixture was filtered, and the solid was washed with methanol to give HETB as a white solid (3.2 g, yield: 78%). ^{1}H-NMR (500 MHz, CD_3OD): δ 2.92 (2 H, t, *J* = 7.0 Hz, H-7), 4.35 (2 H, t, *J* = 7.0 Hz, H-8), 6.72 (2 H, d, *J* = 8.4 Hz, H-3, 5), 7.03 (2 H, s, H-2′, 6′), 7.10 (2 H, d, *J* = 8.4 Hz, H-2, 6); ^{13}C nuclear magnetic resonance (^{13}C-NMR) (500 MHz, CD_3OD): δ 35.6 (C-7), 67.0 (C-8), 110.3 (C-2′,6′), δ 116.5 (C-3, 5), δ 121.8 (C-1′), δ 130.4 (C-1), 131.2 (C-2, 6), 139.8 (C-4′), 146.7 (C-3′,5′), 157.3 (C-4), 168.7 (C-7′). TLC R_f = 0.7 (EtOAc:Hexanes = 1:1) ppm; ESIMS m/z 289.13 $[M + H]^-$. The spectra and physical properties of the synthetic HETB were consistent with the same compound isolated from *Rhodiola crenulata.* The final compound (HETB) has a purity of at least 95%, as determined by high-performance liquid chromatographic (HPLC) analysis.

2.2. Maltase Activity Assay

Maltase derived from *Saccharomyces cerevisiae* and maltose were obtained from Sigma Chemical Co. (St. Louis, MO, USA). Maltase activity was analyzed utilizing the method described by Li et al. [15]. The reaction mixture comprised 50 μL of phosphate buffer (100 mM, pH 7.0), 20 μL of maltase (0.33 units/mL), and 30 μL of 86.3 mM maltose. Following incubation at 37 °C for 10 min, samples were heated to 100 °C for 10 min. The released glucose was then measured using a glucose assay kit (Sigma Chemical Co., St. Louis, MO, USA).

2.3. Maltase Inhibitory Activity of HETB and the Intermediate Compounds

In this study, we focused on HETB and its intermediate compounds. Inhibitory activity of maltase was assayed by directly dissolving the samples in phosphate buffer (100 mM, pH 7.0). The acarbose and voglibose were used as positive controls. The samples (0–50 μM) were assayed for the maltase inhibitory activity, and the half-maximal inhibitory concentration (IC_{50}) values of samples were calculated as follows:

$$[(A_{\text{without sample}} - A_{\text{with sample}})] \times 100\%/A_{\text{without sample}} = \text{percent inhibition (\%)}$$

2.4. Sucrase Activity Assay

Sucrase derived from *Leuconostoc mesenteroides* and sucrose were obtained from Sigma Chemical Co. (St. Louis, MO, USA). Sucrase activity was analyzed utilizing the method described by Li et al. [15]. The reaction mixture comprised 50 μL of phosphate buffer (100 mM, pH 7.0), 40 μL of 480 mM sucrose, and 10 μL of sucrase (0.33 units/mL). Following incubation at 37 °C for 60 min, the samples were heated to 100 °C for 10 min. The concentrations of glucose were then measured using a glucose assay kit (Sigma Chemical Co., St. Louis, MO, USA) according to a protocol recommended by the manufacturer.

2.5. Sucrase Inhibitory Activity of HETB and the Intermediate Compounds

In this study, we focused on HETB and its intermediate compounds. Inhibition of sucrase activity was assayed by directly dissolving the samples in phosphate buffer (100 mM, pH 7.0). The acarbose and voglibose were used as positive controls. The samples (0–160 μM) were assayed for the sucrase inhibitory activity, and the IC_{50} of samples were calculated as follows:

$$[(A_{\text{without sample}} - A_{\text{with sample}})] \times 100\%/A_{\text{without sample}} = \text{percent inhibition (\%)}$$

2.6. Dixon Plots and Lineweaver-Burk Plots

Lineweaver-Burk plots analysis were performed using the methods proposed by Li et al. [15]. The objective of this analysis was to identify the inhibition modes of HETB, acarbose, and voglibose on maltase and sucrase. Dixon plots were used to determine the inhibition constants.

2.7. Docking Experiments

For maltase, the three-dimensional (3D)-structural model of the *Saccharomyces cerevisiae* maltase (*S. cerevisiae*, α-glucosidase, Protein Data Bank (PDB) code: 3A4A) was used in docking experiments. The model of compound HETB was docked into the active site of maltase based on the binding mode of maltose in *S. cerevisiae* maltase [16]. The Crystallographic Object-Oriented Toolkit (COOT) was used to generate an initial binding pose for the manual docking of HETB within the active site, based on the structure of maltase. Discovery Studio software was used to optimize (i.e., minimize and equilibrate) the model of the *S. cerevisiae* maltase-HETB complex via energy minimization based on the standard dynamic cascade approach. For sucrase, the 3D-structural model of the *Saccharomyces* sucrase (invertase, PDB code: 4EQV) was used in docking experiments [17]. The model of compound HETB was manually docked into the active site of the monomer of sucrase to generate an initial binding pose by the program *Coot*. The initial binding model of HETB was then transferred to the oligomer of sucrase. Discovery Studio software was used to optimize the system via energy minimization. Figures showing the structure of the system were generated using PyMOL (Schrödinger, New York, NY, USA).

3. Results and Discussion

3.1. Synthesis of HETB

Figure 1 illustrates the strategy used to synthesize HETB molecules with a structural scaffold comprising hydroxyl-functionalized phenyl ethylbenzoate. Initially, the hydroxyl protection reaction was performed respectively using 4-(2-hydroxyethyl)phenol 1 and methyl 3,4,5-trihydroxybenzoate 4, with benzyl bromide 2 in the presence of potassium carbonate to obtain protected compounds 3 (Figure S1, Supplementary Materials) and 5 (Figure S2) in good to excellent yields. A subsequent saponification reaction of compound 5 was performed using potassium hydroxide to produce acid 6 (Figure S3). The coupling reaction combining acid 6 with compound 3 led to the formation of ester 7 (Figure S4) in a moderate yield of 54%. Finally, a deprotection reaction was conducted using 10% Pd/C in the presence of hydrogen to gefnerate the desired HETB (Figure S5) in a good yield (78%).

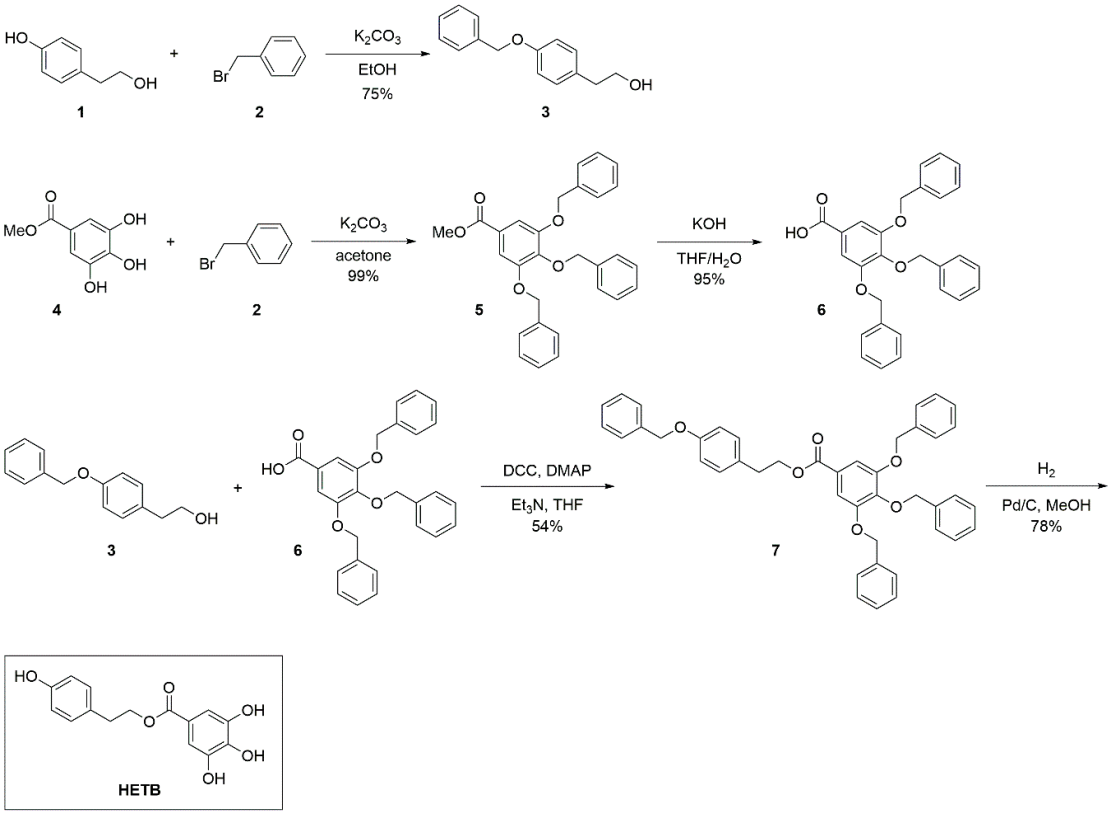

Figure 1. Chemical synthesis of 2-(4-hydroxyphenyl)ethyl 3,4,5-trihydroxybenzoate (HETB).

3.2. Maltase and Sucrase Inhibitory Activity of Compounds 1–7 *and HETB*

Carbohydrate digestion and the transport of monosaccharides into enterocytes can be attenuated by inhibiting sucrase and maltase activity [18]. Inhibition of maltase and sucrase retards the arrival of D-glucose from starch, which results in reduced postprandial plasma glucose concentrations [6]. Therefore, the inhibition of sucrase and maltase by the compounds 1–7 and HETB was investigated. As shown in Figure 2, HETB exhibited significantly higher inhibitory activity on maltase in comparison with compounds 1–7. The addition of 50 μM of inhibitory compounds had the following effects on the inhibition of maltase activity: HETB (71.0%) and compounds 1–7 (8.8%, 10.6%, 18.5%, 24.3%, 26.4%, 19.8%, and 12.7%, respectively) (Figure 2A). Clearly, HETB had the most pronounced inhibitory effects. In a previous study, HETB was shown to have significant inhibitory effects on tyrosinase (IC_{50} = 14.50 μM) and α-glucosidase (IC_{50} = 4.77 μM) activities [13,19]. Since sucrase is involved in intestinal digestion, it is important for the control of blood glucose concentrations and suppression of postprandial hyperglycemia [8]. HETB and compounds 1–7 were also shown to have similar effects on sucrase. The addition of 40 μM of inhibitory compounds had the following effects on the inhibition of sucrase activity: HETB (83.7%) and compounds 1–7 (6.4%, 14.8%, 18.9%, 20.6%, 27.7%, 30.3%, and 20.7%, respectively) (Figure 2B). Again, HETB had the most pronounced inhibitory effects on sucrase. This is a clear demonstration that HETB could be used as a maltase and/or sucrase inhibitor.

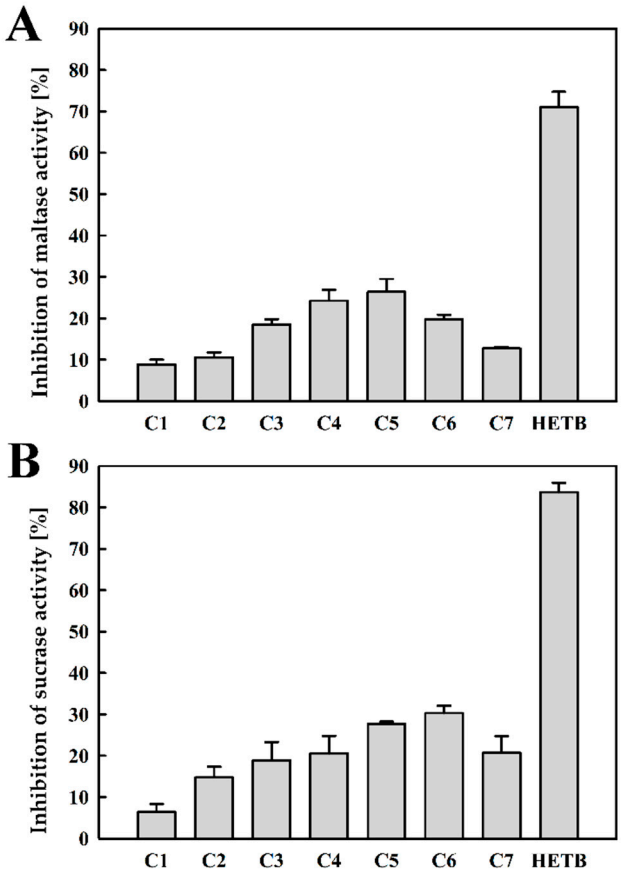

Figure 2. Inhibition of maltase (**A**) and sucrase (**B**) by compounds 1–7 and HETB at concentrations: 50 μM for maltase inhibition and 40 μM for sucrase inhibition. Data are presented as means of three independent determinations ± standard deviation (SD).

3.3. Maltase and Sucrase Inhibitory Activity of Acarbose, Voglibose, and HETB

Acarbose and voglibose have the greatest known inhibitory activity of sucrase and maltase, and HETB showed remarkable inhibitory effects on both sucrase and maltase [20,21]. Therefore, the sucrase and maltase inhibitory activities of HETB were compared with acarbose and voglibose. As shown in Figure 3A, the inhibition of maltase activity increased significantly with the addition of acarbose, voglibose, and HETB. The inhibition levels of maltase by acarbose, voglibose, and HETB at 40 μM were 17.8%, 28.2%, and 64.9%, respectively. The IC_{50} of acarbose, voglibose, and HETB were 133.22 ± 1.67, 77.50 ± 0.44, and 29.96 ± 3.06 μM, respectively. According to the above results, the IC_{50} of three inhibitors displayed the following order: HETB < voglibose < acarbose. In the previous study, the voglibose inhibitory activity on α-glucosidase was stronger than acarbose [22]. These results indicate that HETB showed higher inhibitory activity on maltase than voglibose and acarbose.

Furthermore, the inhibition of sucrase activity increased significantly with the addition of acarbose, voglibose, and HETB. The inhibition levels of sucrase by acarbose, voglibose, and HETB at 30 μM were 17.9%, 18.5%, and 56.7%, respectively (Figure 3B). The IC_{50} of acarbose, voglibose, and HETB were 114.32 ± 3.76, 108.54 ± 2.63, and 26.75 ± 2.54 μM, respectively. According to the above results, the IC_{50} of these inhibitors displayed the following order: HETB < voglibose < acarbose. In a report by Dabhi et al. [23], voglibose was shown to outperform acarbose in inhibiting α-glucosidase activity. In the current study, HETB was shown to outperform voglibose and acarbose in inhibiting sucrase activity.

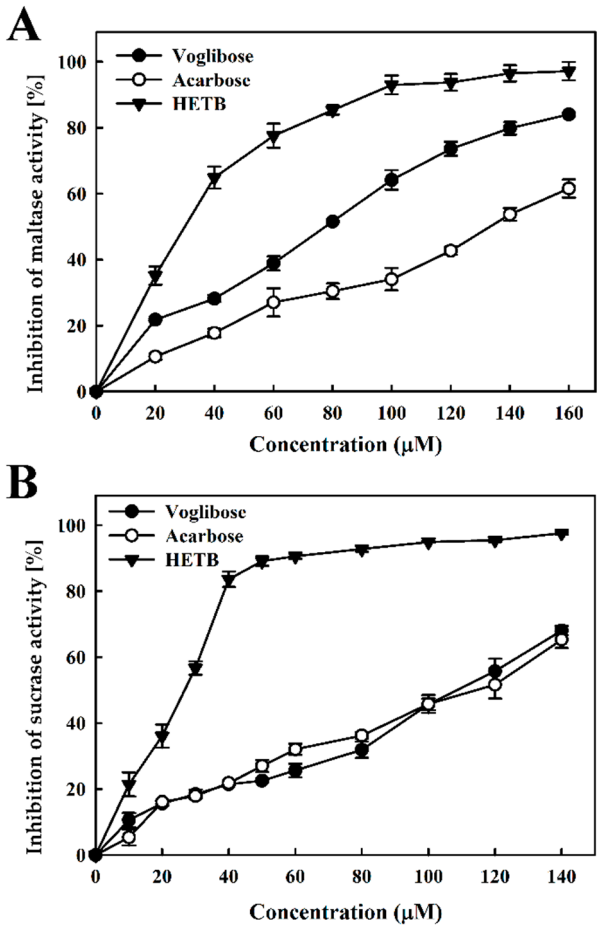

Figure 3. Inhibition of maltase (**A**) and sucrase (**B**) by acarbose, voglibose, and HETB at different concentrations. Data are presented as means of three independent determinations ± SD.

3.4. Kinetics of Maltase Inhibition by Acarbose, Voglibose, and HETB

The kinetics of inhibition of maltase by acarbose, voglibose, and HETB were evaluated. The *Km* of maltase was 1.01 mM in this investigation. Rolfsmeier and Blump reported that the *Km* value of maltase activity was 0.91 mM [24]. As shown in Figure 4, Lineweaver-Burk plots of acarbose, voglibose, and HETB were generated. The straight lines intersecting the *Y*-axis in the Lineweaver-Burk plots (Figure 4A–C) indicate that acarbose, voglibose, and HETB are competitive inhibitors. Several competitive maltase inhibitors have been reported. It appears that quercetin-3-*O*-glucoside derived from rutin is a competitive inhibitor against maltase, with an inhibition constant (*Ki*) of 142 μM [25]. In the previous study, both acarbose and voglibose were competitive inhibitors of maltase [26,27], and the results are consistent with ours. Dixon plots of acarbose, voglibose, and HETB on maltase were also evaluated. The Dixon plot also indicated that acarbose, voglibose, and HETB were competitive inhibitors of maltase, and the *Ki* values were 96.90 ± 0.48, 45.53 ± 0.69, and 37.74 ± 0.28 μM, respectively (Figure 4D–F). The term *Ki* refers to the equilibrium constant of a reversible combination of an enzyme with a competitive inhibitor. The value of *Ki* is usually calculated for a competitive system using the Michaelis equation. The *Ki* values were as follows: HETB < voglibose < acarbose. From our results above, either the IC_{50} or *Ki* values, HETB has better inhibition activity and binding affinities to maltase than voglibose and acarbose. The values of *Ki*' and *Ki* are the equilibrium constant for the binding of the inhibitor to the maltose-maltase complex and maltase, respectively. In this case, voglibose, acarbose, and HETB are competitive inhibitors, such that there is no intersection in the Dixon plot (i.e., the lines are parallel). As a result, it is not possible to obtain the *Ki*' values for acarbose, voglibose, or HETB using the Dixon plot (Figure 4D–F). Maltose could be hydrolyzed to glucose by maltase,

while HETB prevents maltase activity. The value *Ki* is the dissociation constant of the maltase-inhibitor complex. Our results indicate that HETB (*Ki* = 37.74 ± 0.28 μM) is a competitive inhibitor of maltase, which competes with maltose for the active site of maltase to form a maltase-HETB complex. Finally, HETB displayed a strong inhibitory effect on maltase.

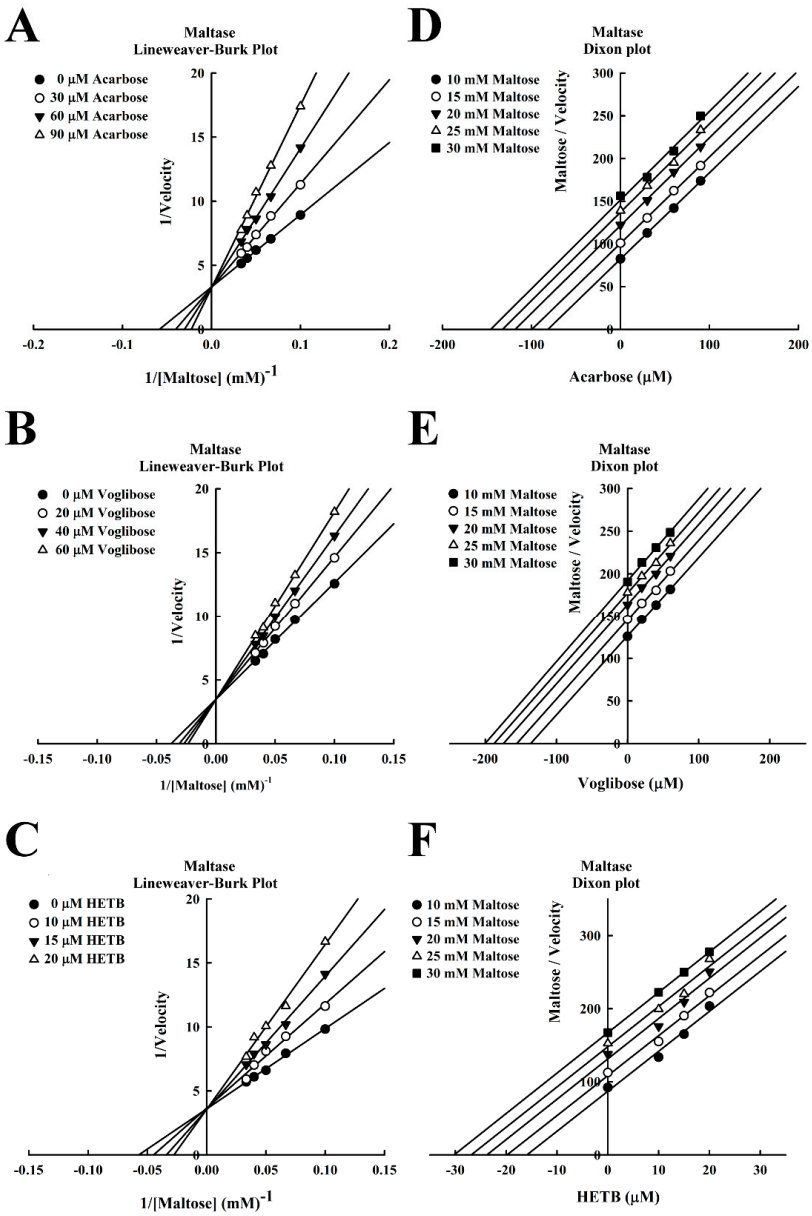

Figure 4. Lineweaver-Burk (**A**–**C**) and Dixon plots (**D**–**F**) of inhibitory effect of maltase inhibitors on maltase. (**A**) Acarbose, (**B**) Voglibose, (**C**) HETB, and (**D**) Acarbose, (**E**) Voglibose, (**F**) HETB. Each sample was analyzed in triplicate.

3.5. Kinetics of Sucrase Inhibition by Acarbose, Voglibose, and HETB

The inhibition kinetics of inhibition of sucrase by acarbose, voglibose and HETB [28] were also evaluated. The Michaelis constant (*Km*) of sucrase was 100.4 mM in this investigation. Houck et al. [29] reported that the *Km* value of maltase activity was 93.0 mM. Lineweaver-Burk plots of acarbose, voglibose, and HETB were generated (Figure 5). Acarbose, voglibose, and HETB have a similar inhibition mode on maltase. As shown in Figure 5A–C, the Lineweaver-Burk plots of acarbose, voglibose, and HETB produced straight lines intersecting the *Y*-axis. This is a clear indication that

these compounds were competitive inhibitors. As previously mentioned, acarbose and voglibose were competitive inhibitors of sucrase [30,31]. Several competitive sucrase inhibitors have been reported. It appears that valienamine is a competitive inhibitor of sucrase activity, with an inhibition constant *Ki* of 770 μM [8]. Dixon plots of acarbose, voglibose, and HETB on sucrase were also evaluated. Dixon plots also indicated that acarbose, voglibose, and HETB were competitive inhibitors of sucrase, and the *Ki* values were 93.20 ± 0.90, 84.49 ± 0.44, and 29.00 ± 0.97 μM, respectively (Figure 5D–F). The *Ki* values were as follows: HETB < voglibose < acarbose. According to our results above, either the IC_{50} or *Ki* values, HETB has better inhibitory activity and binding affinities to sucrase than acarbose and voglibose. Sucrase inhibitors prevent the sucrase activity, while the sucrase could hydrolyze sucrose to glucose. *K*i is the dissociation constant of the inhibitor-sucrase complex. Our results indicate that HETB (*Ki* = 29.00 ± 0.97 μM) acts as a competitive inhibitor of sucrase activity by competing with sucrose for the active site of sucrase to form a sucrase-HETB complex. Finally, HETB exhibited significant inhibitory activity on sucrase.

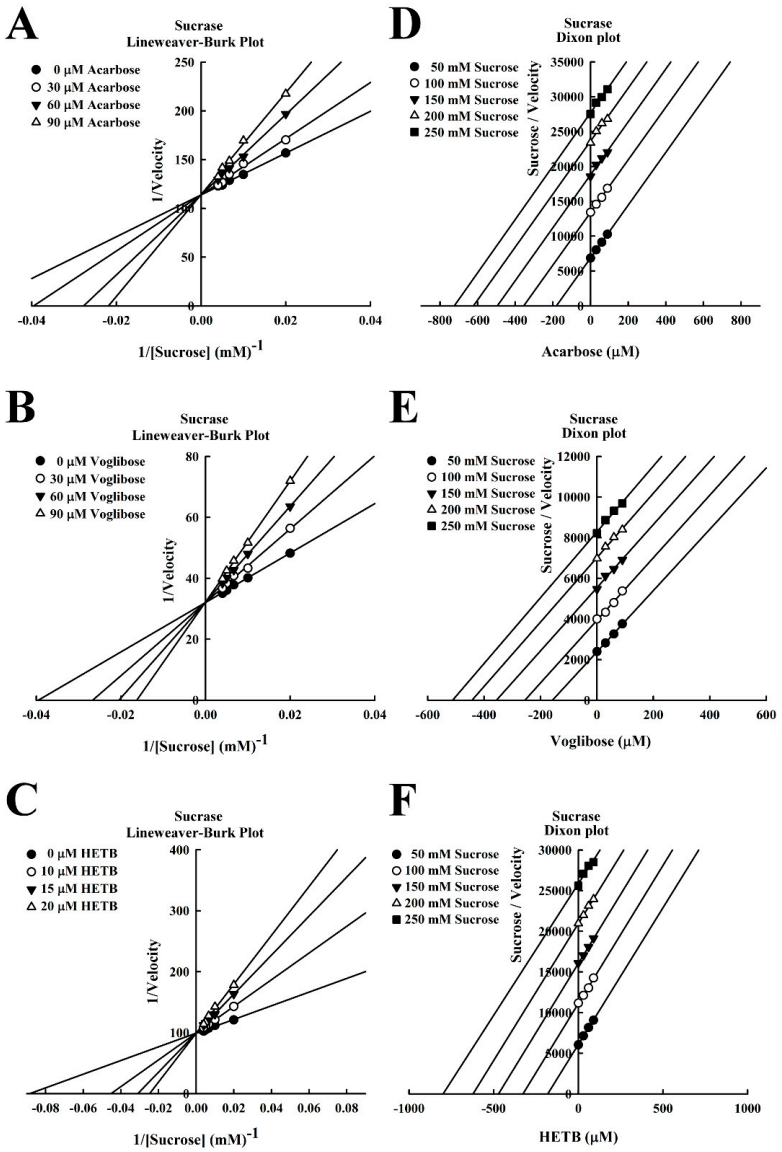

Figure 5. Lineweaver-Burk (**A**–**C**) and Dixon plots (**D**–**F**) of inhibitory effect of sucrase inhibitors on sucrase. (**A**) Acarbose, (**B**) Voglibose, (**C**) HETB, and (**D**) Acarbose, (**E**) Voglibose, (**F**) HETB. Each sample was analyzed in triplicate.

3.6. Molecular Docking of HETB with Maltase and Sucrase

Molecular modeling of HETB and maltase was conducted. As shown in Figure 6, the docking experiments were based on the maltose binding model of *S. cerevisiae* maltase. The active site of maltase includes three catalytic acidic residues: Asp 215, Asp 352, and Glu 277. Our binding model of HETB revealed that Glu 277 is indeed involved in the interactions between maltase and HETB. The proposed structural model of maltase-HETB complex is shown in Figure 6A, which is the 3D-structural model of maltase bound to HETB. The maltase, HETB, and oxygen atoms are respectively indicated in green, light blue, and red. Figure 6B presents a close-up view of the maltase-HETB complex. The stick model in the figure indicates the residues that may be involved in the interactions of compound binding and the dashed lines (magenta) indicate the hydrogen-bond interactions. For HETB, there are five residues (Ser 240, Asp 242, Glu 277, Arg 315, and Asn 350) that form five hydrogen bonds with the compound. Among these residues, Glu 277 is the catalytic acidic residue in the active site of maltase that is involved in the binding of HETB.

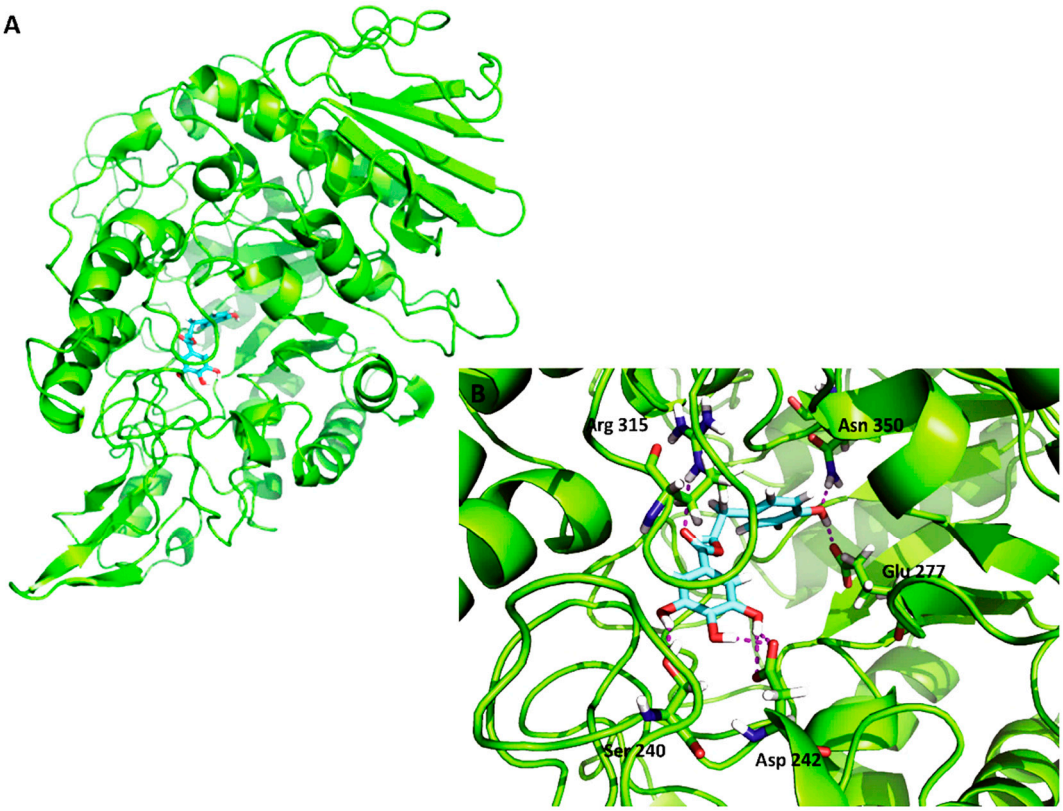

Figure 6. Proposed structural model of maltase-HETB complex. (**A**) HETB, maltase, and oxygen atoms are shown in light blue, green, and red, respectively. (**B**) The nitrogen atoms, oxygen atoms, and hydrogen atoms are labeled in blue, red, and white, respectively.

Molecular modeling of HETB and sucrase was also conducted. As shown in Figure 7, docking experiments were based on the sucrose binding model of *Saccharomyces* sucrase. The binding model of HETB showed that seven residues (Asn 114, Glu 148, Gln 201, Asn 228, Gln 381, Ile 383, and Ser 412) formed seven hydrogen bonds with the compound. The proposed structural model of sucrase-HETB complex is shown in Figure 7A, which is the 3D-structural model of HETB bound to the oligomeric form of *Saccharomyces* sucrase. The monomers of sucrase are shown in different colors. As shown in Figure 7B, two monomers of sucrase are shown in green (monomer 1) and light blue (monomer 2), while the HETB is shown in orange. The sucrase-HETB complex is formed between HETB and monomer 1. Monomer 1 of sucrase and HETB are shown in green and orange, respectively (Figure 7C).

Figure 7D presents a close-up view of the sucrase-HETB complex. The stick model in the figure indicates the residues that may be involved in compound binding and the dashed lines (magenta) indicate the hydrogen-bonding interactions. Hydrogen atoms, nitrogen atoms, and oxygen atoms are respectively indicated in white, blue, and red. Two monomers of sucrase are presented in green (monomer 1) and light blue (monomer 2). HETB is shown in orange. For HETB, there are seven residues (Asn 114, Glu 148, Gln 201, Asn 228, Gln 381, Ile 383, and Ser 412) that formed seven hydrogen bonds with the compound.

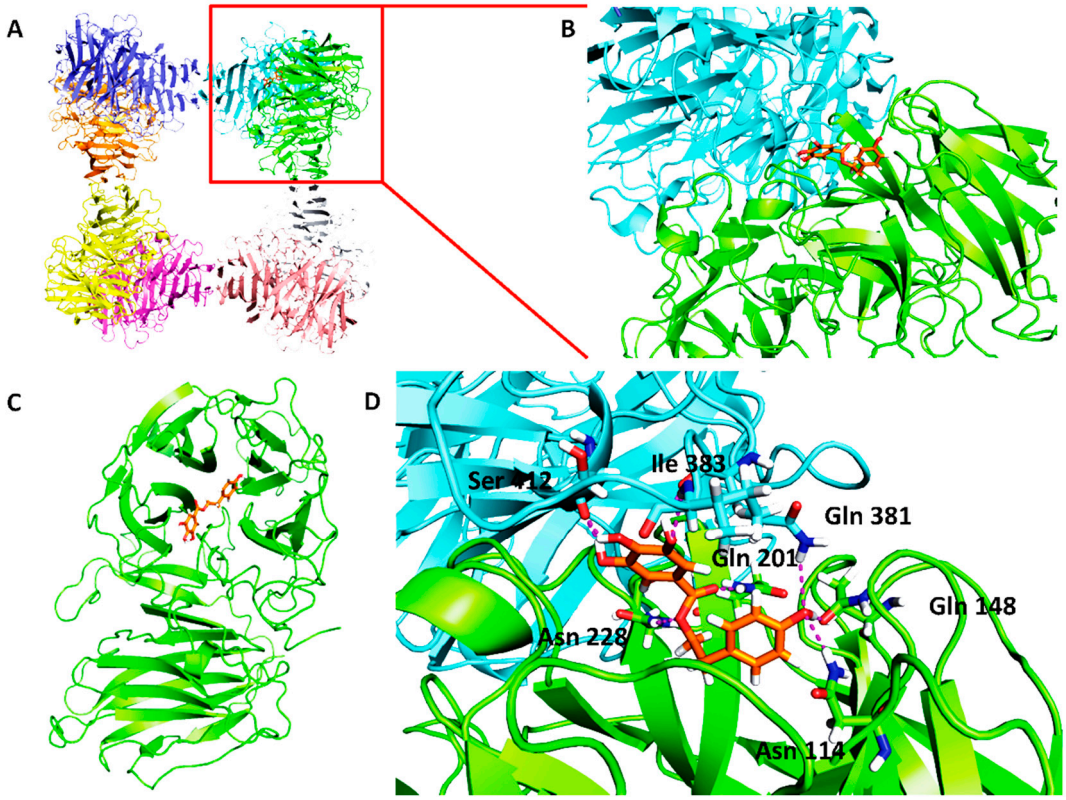

Figure 7. Proposed structural model of sucrase-HETB complex. (**A**) Oligomeric form of *Saccharomyces* sucrase. (**B**) Two monomers of sucrase are shown in green (monomer 1) and light blue (monomer 2). HETB is shown in orange. (**C**) Monomer 1 is shown in green and HETB is shown in orange. (**D**) Two monomers of sucrase are shown in green (monomer 1) and light blue (monomer 2). HETB is shown in orange.

4. Conclusions

Acarbose, voglibose, and HETB are competitive inhibitors of sucrase and maltase activities. The IC_{50} of three inhibitors displayed the following order: HETB < voglibose < acarbose. HETB was a competitive inhibitor of maltase and sucrase, and the *Ki* values were as follows: HETB < voglibose < acarbose. In a molecular docking study, we revealed the HETB binding in active sites of sucrase and maltase by means of hydrogen interactions. This is a clear indication of the potential of HETB in preventing hyperglycemia due to the inhibition of maltase and sucrase activities. Our results suggest that HETB is a good candidate for the treatment of diabetes mellitus and is worthy of further assessment in in vivo studies.

Supplementary Materials: The following are available online at http://www.mdpi.com/2227-9717/8/12/1603/s1.

Author Contributions: Formal Analysis, Data Curation, Preparation of the Research Work, Y.-H.C.; Writing, Data Analysis, W.-T.L.; Software, Validation, J.-H.L.; Investigation of the Study, and contribution to Review and Editing, J.-F.H. All authors have read and agreed to the published version of the manuscript.

Funding: This research was funded by the Ministry of Science and Technology (MOST) in Taiwan, grant number MOST 109-2221-E-030-003-MY2, and The APC was funded by the Ministry of Science and Technology (MOST) and Fu Jen Catholic University.

Acknowledgments: We thank the Ministry of Science and Technology (MOST) in Taiwan for grant support (Grant No. MOST 109-2221-E-030-003-MY2).

Conflicts of Interest: The authors declare no conflict of interest.

References

1. Vinodhini, S.; Rajeswari, V.D. Exploring the antidiabetic and anti-obesity properties of *Samanea saman* through in vitro and in vivo approaches. *J. Cell Biochem.* **2019**, *120*, 1539–1549. [CrossRef] [PubMed]
2. Adisakwattana, S.; Chantarasinlapin, P.; Thammarat, H.; Yibchok-Anun, S. A series of cinnamic acid derivatives and their inhibitory activity on intestinal alpha-glucosidase. *J. Enzyme Inhib. Med. Chem.* **2009**, *24*, 1194–1200. [CrossRef] [PubMed]
3. Rabasa-Lhoret, R.; Chiasson, J.L. Potential of alpha-glucosidase inhibitors in elderly patients with diabetes mellitus and impaired glucose tolerance. *Drugs Aging* **1998**, *13*, 131–143. [CrossRef] [PubMed]
4. Benalla, W.; Bellahcen, S.; Bnouham, M. Antidiabetic medicinal plants as a source of alpha glucosidase inhibitors. *Curr. Diabetes Rev.* **2010**, *6*, 247–254. [CrossRef] [PubMed]
5. Adisakwattana, S.; Ruengsamran, T.; Kampa, P.; Sompong, W. In vitro inhibitory effects of plant-based foods and their combinations on intestinal α-glucosidase and pancreatic α-amylase. *BMC Complement. Altern. Med.* **2012**, *12*, 110. [CrossRef]
6. Southgate, D.A. Digestion and metabolism of sugars. *Am. J. Clin. Nutr.* **1995**, *62*, 203S–210S. [CrossRef]
7. Ryu, H.J.; Seo, E.S.; Kang, H.K.; Kim, Y.M.; Kim, D. Expression, purification, and characterization of human intestinal maltase secreted from *Pichia pastoris*. *Food Sci. Biotechnol.* **2011**, *20*, 561–565. [CrossRef]
8. Zheng, Y.G.; Shentu, X.P.; Shen, Y.C. Inhibition of porcine small intestinal sucrase by valienamine. *J. Enzyme Inhib. Med. Chem.* **2005**, *20*, 49–53. [CrossRef] [PubMed]
9. Girish, T.K.; Pratape, V.M.; Prasada Raoa, U.J.S. Nutrient distribution, phenolic acid composition, antioxidant and alpha-glucosidase inhibitory potentials of black gram (*Vigna mungo* L.) and its milled by-products. *Food Res. Int.* **2012**, *46*, 370–377. [CrossRef]
10. Suzuki, Y.A.; Murata, Y.; Inui, H.; Sugiura, M.; Nakano, Y. Triterpene glycosides of *Siraitia grosvenori* inhibit rat intestinal maltase and suppress the rise in blood glucose level after a single oral administration of maltose in rats. *J. Agric. Food Chem.* **2005**, *53*, 2941–2946. [CrossRef] [PubMed]
11. Sugihara, H.; Nagao, M.; Harada, T.; Nakajima, Y.; Tanimura-Inagaki, K.; Okajima, F.; Tamura, H.; Inazawa, T.; Otonari, T.; Kawakami, M.; et al. Comparison of three α-glucosidase inhibitors for glycemic control and bodyweight reduction in Japanese patients with obese type 2 diabetes. *J. Diabetes Investig.* **2014**, *23*, 206–212. [CrossRef] [PubMed]
12. Taira, M.; Takasu, N.; Komiya, I.; Taira, T.; Tanaka, H. Voglibose administration before the evening meal improves nocturnal hypoglycemia in insulin-dependent diabetic patients with intensive insulin therapy. *Metabolism* **2000**, *49*, 440–443. [CrossRef]
13. Chu, Y.H.; Wu, S.H.; Hsieh, J.F. Isolation and characterization of α-glucosidase inhibitory constituents from *Rhodiola crenulata*. *Food Res. Int.* **2014**, *57*, 8–14. [CrossRef]
14. Akkarachiyasit, S.; Charoenlertkul, P.; Yibchok-Anun, S.; Adisakwattana, S. Inhibitory activities of cyanidin and its glycosides and synergistic effect with acarbose against intestinal α-glucosidase and pancreatic α-amylase. *Int. J. Mol. Sci.* **2010**, *11*, 3387–3396. [CrossRef] [PubMed]
15. Li, W.T.; Chuang, Y.H.; Hsieh, J.F. Characterization of maltase and sucrase inhibitory constituents from *Rhodiola crenulata*. *Foods* **2019**, *8*, 540. [CrossRef]
16. Yamamoto, K.; Miyake, H.; Kusunoki, M.; Osaki, S. Crystal structures of isomaltase from *Saccharomyces cerevisiae* and in complex with its competitive inhibitor maltose. *FEBS J.* **2010**, *277*, 4205–4214. [CrossRef]
17. Sainz-Polo, M.A.; Ramírez-Escudero, M.; Lafraya, A.; González, B.; Marín-Navarro, J.; Polaina, J.; Sanz-Aparicio, J. Three-dimensional structure of *Saccharomyces* invertase: Role of a non-catalytic domain in oligomerization and substrate specificity. *J. Biol. Chem.* **2013**, *288*, 9755–9766. [CrossRef]
18. Hanhineva, K.; Törrönen, R.; Bondia-Pons, I.; Pekkinen, J.; Kolehmainen, M.; Mykkänen, H.; Poutanen, K. Impact of dietary polyphenols on carbohydrate metabolism. *Int. J. Mol. Sci.* **2010**, *11*, 1365–1402. [CrossRef]

19. Lee, C.W.; Son, E.M.; Kim, H.S.; Xu, P.; Batmunkh, T.; Lee, B.J.; Koo, K.A. Synthetic tyrosyl gallate derivatives as potent melanin formation inhibitors. *Bioorg. Med. Chem. Lett.* **2007**, *17*, 5462–5464. [CrossRef]
20. Hwang, I.G.; Kim, H.Y.; Woo, K.S.; Hong, J.T.; Hwang, B.Y.; Jung, J.K.; Lee, J.; Jeong, H.S. Isolation and characterisation of an α-glucosidase inhibitory substance from fructose-tyrosine Maillard reaction products. *Food Chem.* **2011**, *127*, 122–126. [CrossRef]
21. Juretić, D.; Bernik, S.; Cop, L.; Hadzija, M.; Petlevski, R.; Lukac-Bajalo, J. Short-term effect of acarbose on specific intestinal disaccharidase activities and hyperglycaemia in CBA diabetic mice. *J. Anim. Physiol. Anim. Nutr. (Berl.)* **2003**, *87*, 263–268. [CrossRef] [PubMed]
22. Asano, N. Glycosidase inhibitors: Update and perspectives on practical use. *Glycobiology* **2003**, *13*, 93R–104R. [CrossRef] [PubMed]
23. Dabhi, A.S.; Bhatt, N.R.; Shah, M.J. Voglibose: An alpha glucosidase inhibitor. *J. Clin. Diagn. Res.* **2013**, *7*, 3023–3027. [PubMed]
24. Rolfsmeier, M.; Blum, P. Purification and characterization of a maltase from the extremely thermophilic crenarchaeote *Sulfolobus solfataricus*. *J. Bacteriol.* **1995**, *177*, 482–485. [CrossRef]
25. Lee, Y.S.; Huh, J.Y.; Nam, S.H.; Kim, D.; Lee, S.B. Synthesis of quercetin-3-*O*-glucoside from rutin by *Penicillium decumbens* naringinase. *J. Food Sci.* **2013**, *78*, C411–C415. [CrossRef]
26. Gao, H.; Kawabata, J. α-Glucosidase inhibition of 6-hydroxyflavones. Part 3: Synthesis and evaluation of 2,3,4-trihydroxybenzoyl-containing flavonoid analogs and 6-aminoflavones as α-glucosidase inhibitors. *Bioorg. Med. Chem.* **2005**, *13*, 1661–1671. [CrossRef]
27. Fisman, E.Z.; Tenenbaum, A.; Motro, M.; Adler, Y. Oral antidiabetic therapy in patients with heart disease. A cardiologic standpoint. *Herz* **2004**, *29*, 290–298. [CrossRef]
28. Tillekeratne, L.M.; Sherette, A.; Fulmer, J.A.; Hupe, L.; Hupe, D.; Gabbara, S.; Peliska, J.A.; Hudson, R.A. Differential inhibition of polymerase and strand-transfer activities of HIV-1 reverse transcriptase. *Bioorg. Med. Chem. Lett.* **2002**, *12*, 525–528. [CrossRef]
29. Houck, C.M.; Pear, J.R.; Elliott, R.; Perchorowicz, J.T. Isolation of DNA encoding sucrase genes from *Streptococcus salivarius* and partial characterization of the enzymes expressed in *Escherichia coli*. *J. Bacteriol.* **1987**, *169*, 3679–3684. [CrossRef]
30. Park, J.M.; Bong, H.Y.; Jeong, H.I.; Kim, Y.K.; Kim, J.Y.; Kwon, O. Postprandial hypoglycemic effect of mulberry leaf in Goto-Kakizaki rats and counterpart control Wistar rats. *Nutr. Res. Pract.* **2009**, *3*, 272–278. [CrossRef]
31. Fisman, E.Z.; Motro, M.; Tenenbaum, A. Non-insulin antidiabetic therapy in cardiac patients: Current problems and future prospects. *Adv. Cardiol.* **2008**, *45*, 154–170. [PubMed]